RSC Advances

ROYAL SOCIETY OF CHEMISTRY

www.rsc.org/advances

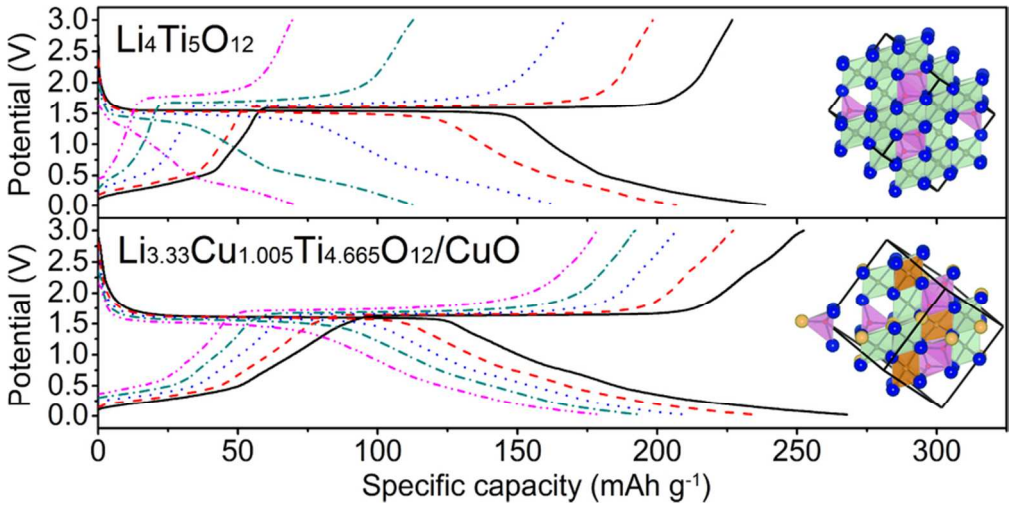

39x19mm (600 x 600 DPI)

RSC Advances

RSCPublishing

COMMUNICATION

One-step fabrication of a $Li_{3.33}Cu_{1.005}Ti_{4.665}O_{12}$/CuO composite for lithium-ion batteries: a high-performance spinel with *P4₃32* space group and synergistic effect of substituting and compositing†

Cite this: DOI: 10.1039/x0xx00000x

Received 00th January 2012,
Accepted 00th January 2012

DOI: 10.1039/x0xx00000x

www.rsc.org/

Chunfu Lin,[a] Man On Lai,[a] Henghui Zhou*[b] and Li Lu*[a]

$Li_{3.33}Cu_{1.005}Ti_{4.665}O_{12}$/CuO was fabricated *via* one-step solid-state reaction. $Li_{3.33}Cu_{1.005}Ti_{4.665}O_{12}$ with *P4₃32* space group shows enhanced electronic conductivity and Li^+ ion diffusion coefficient. The Cu particles reduced from CuO during the first lithiation process benefit the electrical conduction between $Li_{3.33}Cu_{1.005}Ti_{4.665}O_{12}$ particles. Consequently, $Li_{3.33}Cu_{1.005}Ti_{4.665}O_{12}$/CuO exhibits a small potential hysteresis and high rate performance.

The great success that lithium-ion batteries (LIBs) have experienced in portable electronic devices is now being extended to large-scale applications, such as electric vehicles (EVs) and hybrid electrical vehicles (HEVs).[1] Common LIBs rely extensively on the use of carbonaceous anodes. However, the carbonaceous anodes cannot satisfy the demand of high power density in EVs/HEVs due to the safety issue arising from the lithium-dendrite formation and growth on the anode surfaces at low working potentials and high charging currents.[2] To solve this safety problem, $Li_4Ti_5O_{12}$ is being intensively studied owing to its relatively high working potential and good cyclic stability.[3] $Li_4Ti_5O_{12}$ has a spinel structure belonged to a cubic system with $Fd\bar{3}m$ space group, as sketched in Fig. 1a.[4] All O^{2-} ions are exclusively distributed at 32e sites, forming a cubic closest packed structure. 75% of Li^+ ions occupy tetrahedral 8a sites, and 25% Li^+ ions together with all Ti^{4+} ions are disordered, filling octahedral 16d sites in a molar ratio of 1:5. In this cubic closest packed structure, the remaining half of the octahedral sites (16c sites) are vacant. Therefore, $Li_4Ti_5O_{12}$ can be denoted as $Li_3^{8a}(LiTi_5)^{16d}O_{12}^{32e}$. The three-dimensional 8a–16c–8a network is identified as Li^+ ion transport pathways. In the lithiation process of $Li_4Ti_5O_{12}$ at ~1.5 V (all potentials in this study refer to Li/Li^+), the three Li^+ ions initially located at 8a sites together with three external Li^+ ions cooperatively transport to 16c sites accompanied by the reduction of three Ti^{4+} ions to Ti^{3+} ions, thereby generating $Li_6^{16c}(LiTi_5)^{16d}O_{12}^{32e}$. When the working potential further decreases until ~0 V, additional two external Li^+ ions intercalate into two thirds of 8a sites and the remaining two Ti^{4+} ions are reduced, which result in a final state of $Li_2^{8a}Li_6^{16c}(LiTi_5)^{16d}O_{12}^{32e}$ and a theoretical capacity of 293 mA h g^{-1}.[5]

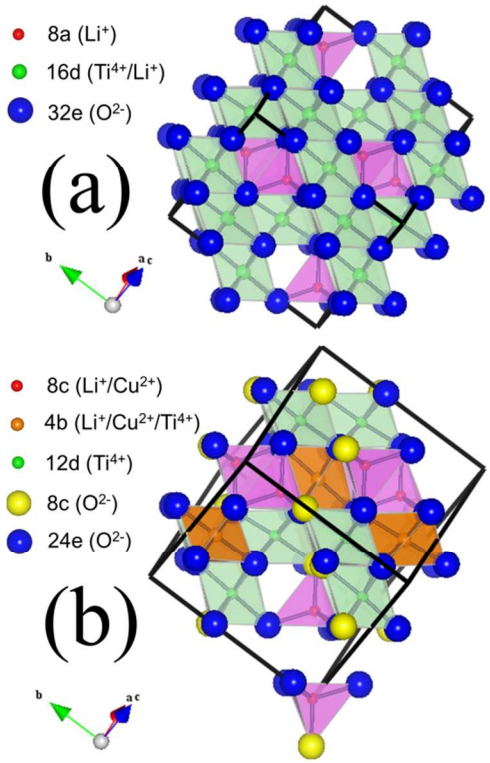

Fig. 1 Schematic representations of spinel structures with (a) $Fd\bar{3}m$ space group and (b) *P4₃32* space group.

P4₃32 space group is another space group in the spinel family. It has 1:3 cation ordering on the octahedral sites. This 1:3

ordering splits 16d sites into 4b and 12 sites, and 32e sites into 8c and 24e sites (Fig. 1b).[6] Such ordered structure has been less well studied. So far, only $LiM_{0.5}Ti_{1.5}O_4$ (M = Co, Zn, Mg, $Co_{0.5}Zn_{0.5}$ and $Mg_{0.5}Zn_{0.5}$) have been developed for the anodes of LIBs.[7–11] They show charge plateaus of ~1.6 V but discharge plateaus of as low as ~0.5 V. These large potential hystereses (~1.1 V), however, greatly limits their electrochemical performances. It is still unclear whether ordered spinel with *P4₃32* space group can outperform disordered spinel with $Fd\bar{3}m$ space group for the anodes of LIBs. Therefore, it is highly desirable to compare these two kinds of spinels from the view of crystal structures and to explore new ordered spinel anode materials with small potential hystereses.

During the lithiation/delithiation process, in order to balance the overall charge, electrons and Li^+ ions synergistically transport in active material particles. Obviously, the whole transport can follow the Cannikin Law, in which the heights of wooden planks represent the values of i) electronic conductivity and ii) Li^+ ion diffusion coefficient in the particles as well as iii) electrical conduction between the particles. Therefore, only the simultaneous improvements of all the three parameters can effectively and significantly facilitate the transport and thus the rate performance. Unfortunately, the intrinsically low electronic conductivity (<1 × 10^{-13} S cm^{-1}) and sluggish Li^+ ion diffusion coefficient (~10^{-12} cm^2 s^{-1}) of $Li_4Ti_5O_{12}$ greatly limit its rate performance.[12,13] Substitution by alien ions can effectively modify the crystal structure and thus engineer the electronic conductivity and/or Li^+ ion diffusion coefficient of $Li_4Ti_5O_{12}$ particles, but cannot increase the electrical conduction between the particles.[12–21] In contrast, compositing with a conductive phase can enhance the electrical conduction between the particles but cannot alter the intrinsic (electronic and ionic) conductivity.[22–29] Clearly, the single use of either strategy cannot remarkably improve the rate performance. Therefore, it is highly necessary to develop effective strategies to significantly improve the rate performance through simultaneously enhance the electronic conductivity and Li^+ ion diffusion coefficient of the particles as well as the electrical conduction between the particles.

To achieve the above goals, we have fabricated Cu^{2+}-substituted $Li_4Ti_5O_{12}$ composited with CuO *via* one-step solid-state reaction. The Cu^{2+}-substituted $Li_4Ti_5O_{12}$ exhibits *P4₃32* space group and a small potential hysteresis. This synergistic strategy of Cu^{2+} substituting and CuO compositing simultaneously improves the three parameters above and thus the rate performance of $Li_4Ti_5O_{12}$.

Cu^{2+}-modified $Li_4Ti_5O_{12}$ powders with a designed nominal composition of $LiCu_{0.5}Ti_{1.5}O_4$ were synthesized by one-step solid-state reaction from Li_2CO_3, CuO and TiO_2 with a predetermined molar ratio of Li : Cu : Ti = 1.07 : 0.5 : 1.5. As a comparison, $Li_4Ti_5O_{12}$ was also prepared by the same process expect that the ratio of Li : Cu : Ti = 4.28 : 0 : 5. The observed, calculated, error patterns and Rietveld refinement results for both samples are presented in Fig. 2. The detailed process of the refinements is shown in Electronic Supplementary Information.† All diffraction peaks for $Li_4Ti_5O_{12}$ in Fig. 2a conform to a spinel structure with $Fd\bar{3}m$ space group (JCPDS 26-1198) without any impurity phases. $Li_4Ti_5O_{12}$ has a lattice parameter of 8.3613 Å and negligible non-Li^+ ions in 8a sites, which suggests that the three-dimensional 8a–16c–18a Li^+ ion transport pathways are negligibly blocked.

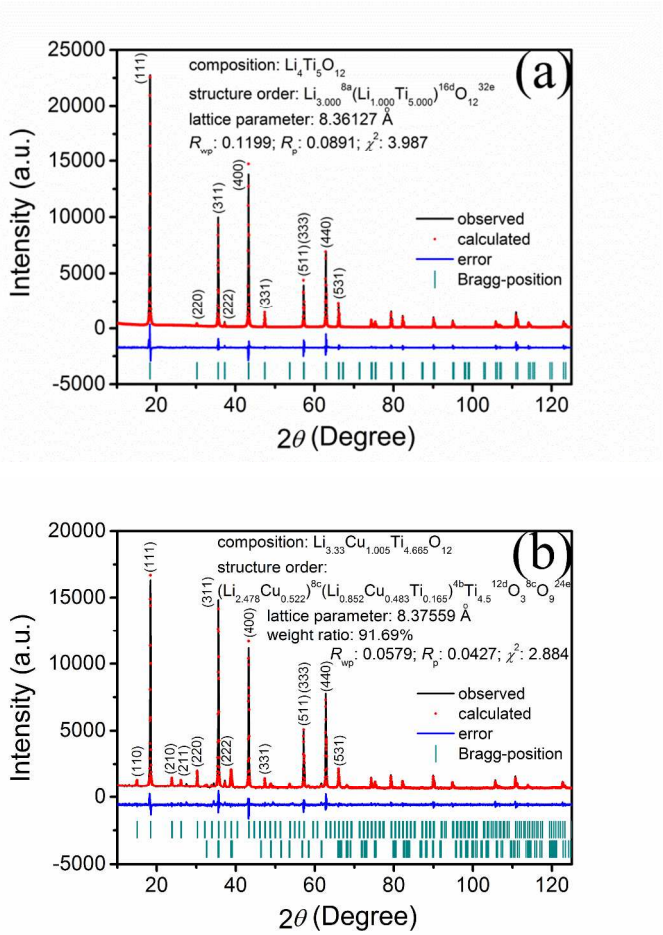

Fig. 2 X-ray diffraction patterns and Rietveld refinement results of (a) $Li_4Ti_5O_{12}$ and (b) $Li_{3.33}Cu_{1.005}Ti_{4.665}O_{12}$/CuO. No all peaks were indexed due to the large number of peaks.

Compared with $Li_4Ti_5O_{12}$, Cu^{2+}-modified $Li_4Ti_5O_{12}$ shows four different features in its structure. Firstly, although its designed nominal composition is $LiCu_{0.5}Ti_{1.5}O_4$, the resultant material is not $LiCu_{0.5}Ti_{1.5}O_4$ but a two-phase composite. The two peaks with considerable intensity at ~39° and ~49° can respectively be identified to be the (111)/(200) and $(20\bar{2})$ peaks of tenorite CuO, which is a Cu-rich phase. All the peaks excluding those of CuO can be indexed as a spinel, which should be a Cu-poor phase. Secondly, this spinel does not possess $Fd\bar{3}m$ space group but *P4₃32* space group since additional peaks (such as (110), (210) and (211) peaks) corresponding to the ordering on the octahedral sites appear. To achieve particle balance and charge neutrality, the spinel is reasonably assigned to $Li_{4-2x}Cu_{3x}Ti_{5-x}O_{12}$, in which every two Li^+ ions and every one Ti^{4+} ion are substituted by three Cu^{2+} ions compared with $Li_4Ti_5O_{12}$. The reasonable Rietveld refinement result (R_{wp} = 0.0579) shows that the *x* value is 0.335, nominal composition is $Li_{3.33}Cu_{1.005}Ti_{4.665}O_{12}$, and weight ratio of $Li_{3.33}Cu_{1.005}Ti_{4.665}O_{12}$ is 91.69±0.06%. Thirdly, the structure

order of the spinel is $(Li_{2.478}Cu_{0.522})^{8c}(Li_{0.852}Cu_{0.483}Ti_{0.165})^{4b}Ti_{4.5}{}^{12d}O_3{}^{8c}O_9{}^{24e}$, suggesting that 17.4% of the tetrahedral 8c sites are occupied by Cu^{2+} ions and thus the three-dimensional Li^+ ion transport pathways are blocked to a certain extend. However, this ratio is much smaller than those of $LiCo_{0.5}Ti_{1.5}O_4$ (45%) and $LiZn_{0.5}Ti_{1.5}O_4$ (50%).[30] Finally, $Li_{3.33}Cu_{1.005}Ti_{4.665}O_{12}$ has a lattice parameter of 8.3756 Å, larger than that of $Li_4Ti_5O_{12}$. The increase can be attributed to the ion-size effect. For $(Li_{2.478}Cu_{0.522})^{8c}(Li_{0.852}Cu_{0.483}Ti_{0.165})^{4b}Ti_{4.5}{}^{12d}O_3{}^{8c}O_9{}^{24e}$, compared with $Li_4Ti_5O_{12}$, 0.552 Li^+ ions (0.59 Å)[31] are substituted by Cu^{2+} ions (0.57 Å) in the tetrahedral sites, while 0.148 Li^+ ions (0.76 Å) and 0.335 Ti^{4+} ions (0.605 Å) are replaced by Cu^{2+} ions (0.73 Å) in the octahedral sites. Since 0.552 × (0.57 – 0.59) + 0.148 × (0.73 – 0.76) + 0.335 × (0.73 – 0.605) = 0.026395 > 0, the increased lattice parameter has been achieved.

Fig. S1a and b† respectively display the morphologies of $Li_4Ti_5O_{12}$ and $Li_{3.33}Cu_{1.005}Ti_{4.665}O_{12}$/CuO. Clearly, both samples have similar morphologies with wide particle-size distributions ranging from less than 100 nm to more than 1000 nm, suggesting that the Cu^{2+} substituting has negligible influences on the morphology and particle size.

The electrochemical performances of $Li_4Ti_5O_{12}$ and $Li_{3.33}Cu_{1.005}Ti_{4.665}O_{12}$/CuO were examined through cyclic voltammetry (CV) at a scan rate of 0.1 mV s^{-1} for four cycles and then successively at 0.3, 0.5 and 0.7 mV s^{-1} for one cycle each, as presented in Fig. 3a and b. In the first cycle of each sample, there is a pair of cathodic/anodic peaks centered at 1.3–1.5/1.6–1.8 V, corresponding to the lithiation/delithiation in empty octahedral sites and the Ti^{4+}/Ti^{3+} redox couple.[5] Moreover, the cathodic/anodic peaks below 0.6 V present the lithiation/delithiation in empty tetrahedral also arising from the Ti^{4+}/Ti^{3+} redox couple.[5] Besides these peaks from the redox couple of Ti^{4+}/Ti^{3+}, additional peaks centered at 2.4–2.6, ~1.1 and ~0.8 V for $Li_{3.33}Cu_{1.005}Ti_{4.665}O_{12}$/CuO were observed in the first cathodic scan, which can be ascribed to the reduction of CuO to CuO_{1-x} ($0<x<0.2$), CuO_{1-x} ($0<x<0.2$) to Cu_2O, and Cu_2O to Cu, respectively.[32] Interestingly, no peaks related to the oxidation of Cu can be detected in the subsequent anodic scan, indicating that CuO was not reproduced and thus Cu was stable in the following cycles.

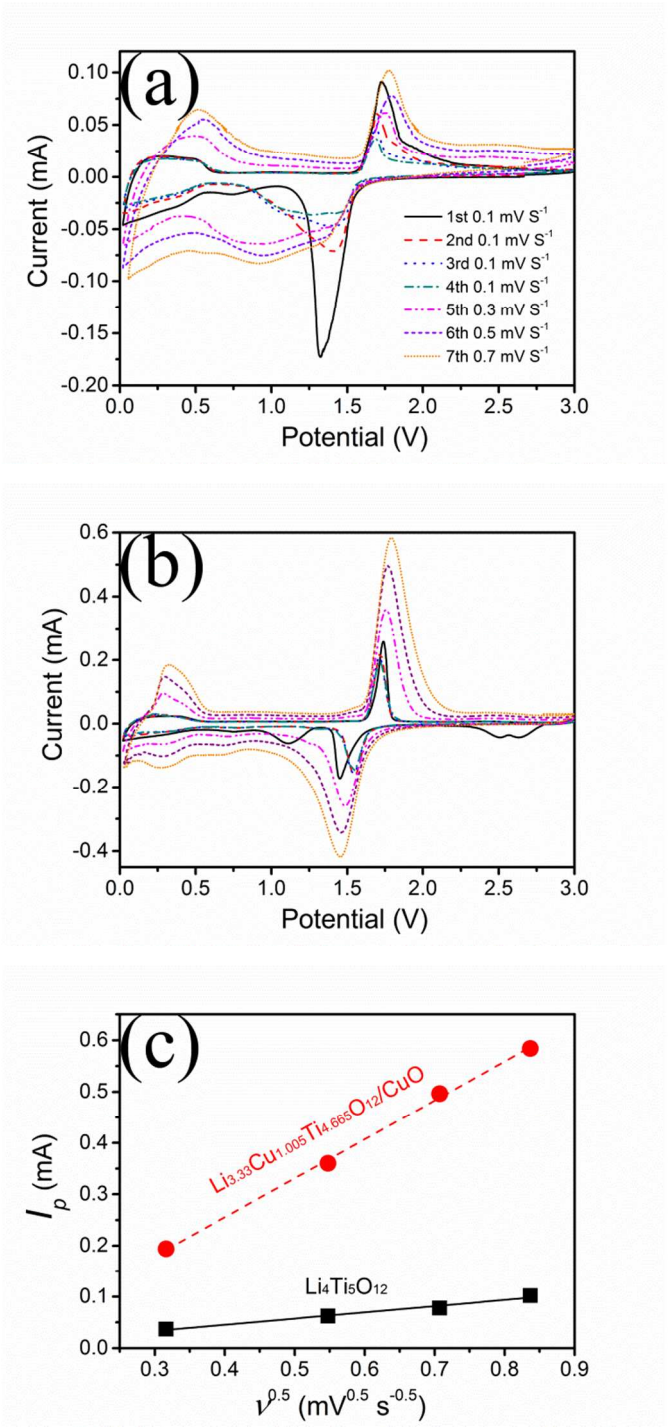

Fig. 3 CVs of (a) $Li_4Ti_5O_{12}$ and (b) $Li_{3.33}Cu_{1.005}Ti_{4.665}O_{12}$/CuO; and (c) relationship between I_p and $\nu^{0.5}$.

From the second cycles at 0.1 mV s^{-1}, $Li_{3.33}Cu_{1.005}Ti_{4.665}O_{12}$/CuO shows stable and well-overlapped cycles with sharp redox peaks at 1.55/1.72 V. In contrast, Cycles 2 through 4 of $Li_4Ti_5O_{12}$ are mismatched, and their peaks centered at ~1.41/~1.70 V are broadened with low peak currents. Obviously, the potential difference of $Li_{3.33}Cu_{1.005}Ti_{4.665}O_{12}$/CuO between the cathodic and anodic peaks is 0.17 V, much smaller than that of $Li_4Ti_5O_{12}$ (0.29 V). The alleviated polarization

together with the intensive and sharp peaks as well as the overlapped cycles in $Li_{3.33}Cu_{1.005}Ti_{4.665}O_{12}$/CuO implies its augment of the mixed (electronic and ionic) conductivity, high reactivity, excellent cycle reversibility and high rate performance. In addition, unlike the previously developed $LiM_{0.5}Ti_{1.5}O_4$ (M = Co, Zn, Mg, $Co_{0.5}Zn_{0.5}$ and $Mg_{0.5}Zn_{0.5}$) showing negligible cathodic peaks at ~1.5 V,[7–11] $Li_{3.33}Cu_{1.005}Ti_{4.665}O_{12}$/CuO exhibits intensive cathodic peaks at ~1.5 V comparable to the anodic peaks at ~1.7 V, suggesting that its electrochemical kinetics is significantly better than those of $LiM_{0.5}Ti_{1.5}O_4$.

Fig. 3c shows that the anodic peak currents I_p are in proportional to the square root of the scan rate $\nu^{0.5}$. Thus, the Li^+ ion diffusion coefficient D can be calculated based on the equation: $I_p = 2.69 \times 10^5\ Sn^{1.5}CD^{0.5}\nu^{0.5}$, where S is the electrode surface area, n, the number of electrons per molecule, and C, the concentration of Li^+ ions.[11] Consequently, the Li^+ ion diffusion coefficient of $Li_{3.33}Cu_{1.005}Ti_{4.665}O_{12}$/CuO is determined to be 3.38×10^{-10} $cm^2\ s^{-1}$, which is 38 times larger than that of $Li_4Ti_5O_{12}$ (8.76×10^{-12} $cm^2\ s^{-1}$). Although the occupancy of some Cu^{2+} ions in 8c sites of $Li_{3.33}Cu_{1.005}Ti_{4.665}O_{12}$ is unfavourable for the Li^+ ion transport, the larger lattice parameter benefits it and may play the dominant role in the entire Li^+ ion transport, leading to the significantly improved Li^+ ion diffusion coefficient of $Li_{3.33}Cu_{1.005}Ti_{4.665}O_{12}$/CuO.

Fig. 4 plots the first and second discharge-charge profiles of $Li_{3.33}Cu_{1.005}Ti_{4.665}O_{12}$/CuO at a current density of 62.5 mA g^{-1}. The first discharge profile exhibits considerable discharge capacities at 2.4–2.6, ~1.1 and ~0.8 V, which correspond to the reduction of CuO to Cu. However, the first charge profile does not show any plateaus related to the oxidation of Cu, and matches well with the second charge profile, indicating that Cu was stable after the first lithiation process. This result is well consistent with the CV analysis. Fig. 5 compares the second discharge-charge profiles of $Li_4Ti_5O_{12}$ and $Li_{3.33}Cu_{1.005}Ti_{4.665}O_{12}$/CuO at various current densities. Similar to $Li_4Ti_5O_{12}$, $Li_{3.33}Cu_{1.005}Ti_{4.665}O_{12}$/CuO shows a discharge plateau of ~1.55 V and charge plateau of ~1.60 V at 62.5 mA g^{-1}. This potential hysteresis of ~0.05 V for $Li_{3.33}Cu_{1.005}Ti_{4.665}O_{12}$/CuO is significantly smaller than those for $LiM_{0.5}Ti_{1.5}O_4$ (~1.1 V) with negligible discharge plateaus above 1 V,[7–11] which infers that the lithiation/delithiation behaviour of $Li_{3.33}Cu_{1.005}Ti_{4.665}O_{12}$ approaches that of $Li_4Ti_5O_{12}$ but differs from those of $LiM_{0.5}Ti_{1.5}O_4$. The polarization of $Li_{3.33}Cu_{1.005}Ti_{4.665}O_{12}$/CuO is obviously smaller than that of $Li_4Ti_5O_{12}$ at both low and high current densities. $Li_{3.33}Cu_{1.005}Ti_{4.665}O_{12}$/CuO delivers a large capacity of 252 mA h g^{-1} at 62.5 mA g^{-1}, which is 25 mA h g^{-1} larger than that of $Li_4Ti_5O_{12}$ (227 mA h g^{-1}). Moreover, $Li_{3.33}Cu_{1.005}Ti_{4.665}O_{12}$/CuO exhibits a much higher rate performance with a high capacity of 179 mA h g^{-1} at 1000 mA g^{-1}, which is 1.5 times larger than that of $Li_4Ti_5O_{12}$ (70 mA h g^{-1}). This rate performance is even comparable to those of nanosized $LiM_{0.5}Ti_{1.5}O_4$, although $Li_{3.33}Cu_{1.005}Ti_{4.665}O_{12}$/CuO has much larger particle sizes (Fig. S1b†) than $LiM_{0.5}Ti_{1.5}O_4$.[7–11] It is also worth noting that this rate performance is obviously better than those of Cu^{2+}-substituted $Li_4Ti_5O_{12}$ and $Li_4Ti_5O_{12}$/CuO, as revealed in Fig. S2.† Such high rate performance can therefore be attributed to the synergistic effect of Cu^{2+} substituting and CuO compositing with these simultaneous improvements. (1) Through the incorporation of Cu^{2+} ions with a $t_{2g}6\ e_g2$ electronic configuration,[33] the free 3d electrons in Cu^{2+} ions are introduced into the spinel crystalline structure, enhancing the electronic conductivity.[34–37] Lin *et al.* reported that the electronic conductivity $Li_{3.7}Cu_{0.45}Ti_{4.85}O_{12}$ was 6.6×10^{-8} S cm^{-1}.[16] Although the real electronic conductivity cannot be accurately measured due to the presence of CuO, it is reasonable to deduce that the electronic conductivity of $Li_{3.33}Cu_{1.005}Ti_{4.665}O_{12}$ is larger than 6.6×10^{-8} S cm^{-1} since it has more Cu^{2+} ions than $Li_{3.7}Cu_{0.45}Ti_{4.85}O_{12}$. The value is at least five orders larger than that of $Li_4Ti_5O_{12}$. (2) $Li_{3.33}Cu_{1.005}Ti_{4.665}O_{12}$/CuO shows an increased Li^+ ion diffusion coefficient, 38 times larger than that of $Li_4Ti_5O_{12}$. (3) The reduced Cu with excellent electrical conductivity can remarkably improve the electrical conduction between the $Li_{3.33}Cu_{1.005}Ti_{4.665}O_{12}$ particles, although the existence of Cu does not favor industrial use. Due to the significantly improved electrochemical kinetics originated from these three improvements, $Li_{3.33}Cu_{1.005}Ti_{4.665}O_{12}$/CuO further exhibits excellent cyclic stability, as displayed in Fig. 6. After 100 cycles at 1000 mA g^{-1}, it still remains a capacity of 177 mA h g^{-1} with only 1.0% capacity loss. This cyclic stability is significantly better than those of $Li_4Ti_5O_{12}$, Cu^{2+}-substituted $Li_4Ti_5O_{12}$ and $Li_4Ti_5O_{12}$/CuO (Fig. 6 and Fig. S3†), which further shows the advantages of this synergistic strategy combining Cu^{2+} substituting and CuO compositing.

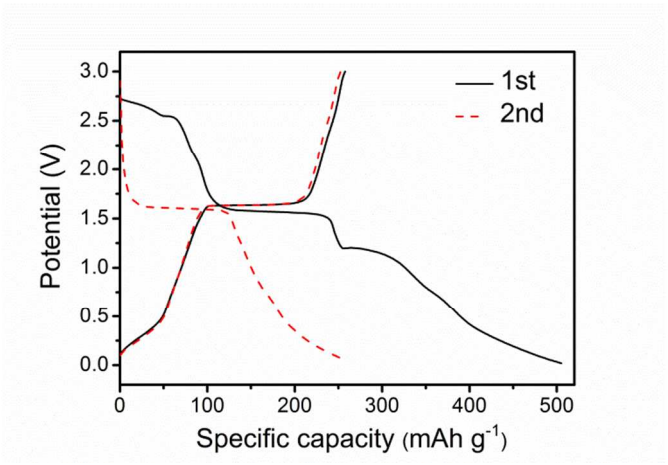

Fig. 4 First and second discharge–charge profiles of $Li_{3.33}Cu_{1.005}Ti_{4.665}O_{12}$/CuO at 62.5 mA g^{-1}. Identical discharge–charge rates were used.

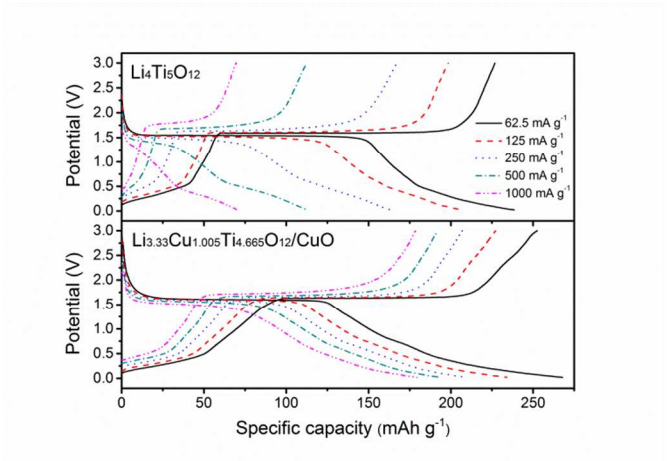

Fig. 5 Second discharge–charge profiles of $Li_4Ti_5O_{12}$ and $Li_{3.33}Cu_{1.005}Ti_{4.665}O_{12}$/CuO at 62.5–1000 mA g^{-1}. Identical discharge–charge rates were used.

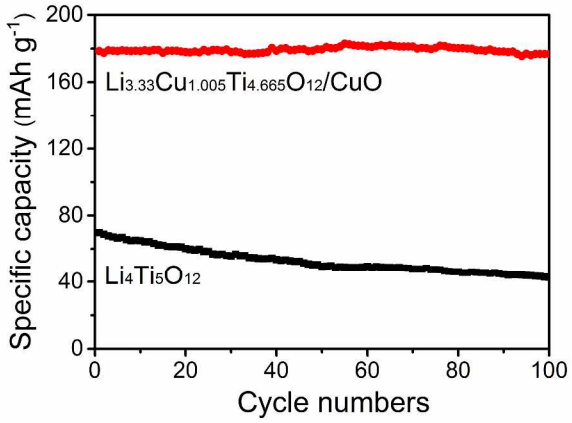

Fig. 6 Cyclic stability of $Li_4Ti_5O_{12}$ and $Li_{3.33}Cu_{1.005}Ti_{4.665}O_{12}$/CuO at 1000 mA g^{-1}. Identical discharge–charge rates were used.

Conclusions

The $Li_{3.33}Cu_{1.005}Ti_{4.665}O_{12}$/CuO composite containing 91.7 wt% spinel $Li_{3.33}Cu_{1.005}Ti_{4.665}O_{12}$ with *P4₃32* space group and 8.3 wt% CuO has been prepared *via* one-step solid-state reaction. Due to the free 3d electrons in Cu^{2+} ions and larger lattice parameter, $Li_{3.33}Cu_{1.005}Ti_{4.665}O_{12}$ reveals significantly higher electronic conductivity and Li^+ ion diffusion coefficient than those of $Li_4Ti_5O_{12}$. CuO is reduced to Cu during the first lithiation process of the composite. However, it is observed that the reduced Cu is unable to be re-oxidized. The reduced Cu, with excellent electrical conductivity, remarkably improves the electrical conduction between the $Li_{3.33}Cu_{1.005}Ti_{4.665}O_{12}$ particles. As a result of this synergistic strategy combining Cu^{2+} substituting and CuO compositing, the composite delivers a high capacity of 179 mA h g^{-1} with capacity retention of 99.0% over 100 cycles at a current density of 1000 mA g^{-1}, while $Li_4Ti_5O_{12}$ only has 70 mA h g^{-1}. In addition, the composite exhibits a fairly small potential hysteresis, which is remarkably smaller than those of $LiM_{0.5}Ti_{1.5}O_4$ (M = Co, Zn, Mg, $Co_{0.5}Zn_{0.5}$ and $Mg_{0.5}Zn_{0.5}$). To the best of our knowledge, $Li_{3.33}Cu_{1.005}Ti_{4.665}O_{12}$ is the first developed titanate-based spinel with *P4₃32* space group possessing a small potential hysteresis and high electrochemical performances for the anodes of LIBs. This work demonstrates that ordered spinels with *P4₃32* space group can have better material properties and electrochemical performances than disordered spinels with $Fd\bar{3}m$ space group.

Acknowledgement

This research is supported by Agency for Science, Technology and Research, Singapore through Singapore–China Joint Research programme (R265-000-442-305 and No.2012DFG52130).

Notes and references

[a] Department of Mechanical Engineering, National University of Singapore, 9 Engineering Drive 1, Singapore 117576, Singapore. E-mail: luli@nus.edu.sg; Fax: +65-67791459; Tel: +65-65162236
[b] College of Chemistry and Molecular Engineering, Peking University, Beijing 100871, PR China. E-mail address: hhzhou@pku.edu.cn; Fax: +86-10-62757908; Tel: +86-10-62757908

† Electronic Supplementary Information (ESI) available: Experimental details, detailed process of Rietveld refinements, FESEM images of $Li_4Ti_5O_{12}$ and $Li_{3.33}Cu_{1.005}Ti_{4.665}O_{12}$/CuO, second discharge–charge profiles of $Li_{3.4}Cu_{0.9}Ti_{4.7}O_{12}$ and $Li_4Ti_5O_{12}$/CuO at 62.5–1000 mA g^{-1}, and cyclic stability of $Li_{3.4}Cu_{0.9}Ti_{4.7}O_{12}$ and $Li_4Ti_5O_{12}$/CuO. See DOI: 10.1039/c000000x/

1 M. Armand and J. M. Tarascon, *Nature*, 2008, **451**, 652.
2 S. S. Zheng, *J. Power Sources*, 2006, **161**, 1385.
3 T. F. Yi, Y. Xie, Q. J. Wu, H. P. Liu, L. J. Jiang, M. F. Ye and R. S. Zhu, *J. Power Sources*, 2012, **214**, 220.
4 J. B. Goodenough and Y. Kim, *Chem. Mater.*, 2010, **22**, 587.
5 H. Ge, N. Li, D. Y. Li, C. S. Dai and D. L. Wang, *J. Phys. Chem. C*, 2009, **113**, 6324.
6 P. Reale, S. Panero, F. Ronci, V. R. Albertini and B. Scrosati, *Chem. Mater.*, 2003, **15**, 3437.
7 Z. S. Hong, X. Z. Zheng, X. K. Ding, L. L. Jiang, M. D. Wei and K. M. Wei, *Energy Environ. Sci.*, 2011, **4**, 1886.
8 Z. S. Hong, T. B. Lan, Y. Z. Zheng, L. L. Jiang and M. D. Wei, *Funct. Mater. Lett.*, 2011, **4**, 65.
9 Z. S. Hong and M. D. Wei, *J. Mater. Chem. A*, 2013, **1**, 4403.
10 Y. X. Yu, Z. S. Hong, L. C. Xia, J. Yang and M. D. Wei, *Electrochim. Acta*, 2013, **88**, 74.
11 L. Wang, Q. Z. Xiao, Z. H. Li, G. T. Lei, L. J. Wu, P. Zhang and J. Mao, *Electrochim. Acta*, 2012, **77**, 77.
12 C. H. Chen, J. T. Vaughey, A. N. Jansen, D. W. Dees, A. J. Kahaian, T. Goacher and M. M. Thackeray, *J. Electrochem. Soc.*, 2001, **148**, A102.
13 C. X. Qiu, Z. Z. Yuan, L. Liu, J. C. Cheng and J. C. Liu, *Chin. J. Chem.*, 2013, **31**, 819.
14 Y. J. Bai, C. Gong, N. Lun and Y. X. Qi, *J. Mater. Chem. A*, 2013, **1**, 89.
15 X. Li, S. H. Tang, M. Z. Qu, P. X. Huang, W. Li and Z. L. Yu, *J. Alloy Compd.*, 2014, **588**, 17.

16 C. F. Lin, B. Ding, Y. L. Xin, F. Q. Cheng, M. O. Lai, L. Lu and H. H. Zhou, *J. Power Sources*, 2014, **248**, 1034.
17 C. F. Lin, M. O. Lai, L. Lu, H. H. Zhou and Y. L. Xin, *J. Power Sources*, 2013, **244**, 272.
18 Q. Y. Zhang, C. L. Zhang, B. Li, D. D. Jiang, S. F. Kang, X. Li and Y. G. Wang, *Electrochim. Acta*, 2013, **107**, 139.
19 S. Sharmila, B. Senthilkumar, V. D. Nithya, K. Vediappan, C. W. Lee and R. K. Selvan, *J. Phys. Chem. Solids*, 2013, **74**, 1515.
20 C. X. Qiu, Z. Z. Yuan. L. Liu, N. Ye and J. C. Liu, *J. Solid State Electrochem.*, 2013, **17**, 841.
21 C. F. Lin, X. Y. Fan, Y. L. Xin, F. Q. Cheng, M. O. Lai, H. H. Zhou and L. Lu, *J. Mater. Chem. A*, 2014, **2**, 9982.
22 D. Yoshikawa, N. Suzuki, Y. Kadoma, K. Ui and N. Kumagai, *Funct. Mater. Lett.*, 2012, **5**, 125001.
23 B. Zhang, Y. Yu, Y. S. Liu, Z. D. Huang, Y. B. He and J. K. Kim, *Nanoscale*, 2013, **5**, 2100.
24 L. F. Shen, C. Z. Yuan, H. J. Luo, X. G. Zhang, K. Xu and F. Zhang, *J. Mater. Chem.*, 2011, **21**, 761.
25 W. Wang, Y. Y. Guo, L. X. Liu, S. X. Wang, X. J. Yang and H. Guo, *J. Power Sources*, 2014, **245**, 624.
26 S. Hao, X. L. Xiao, Z. B. Hu, L. M. Sun, S. B. Han, D. F. Chen and X. F. Liu, *J. Phys. Chem. C*, 2013, **117**, 26889.
27 K. S. Park, A. Benayad, D. J. Kang and S. G. Doo, *J. Am. Chem. Soc.*, 2008, **130**, 14930.
28 S. G. Ri, L. Zhan, Y. Wang, L. H. Zhou, J. Hu and H. L. Liu, *Electrochim. Acta*, 2013, **109**, 389.
29 C. T. Hsieh, B. S. Chang, J. Y. Lin and R. S. Juang, *J. Alloys Compd.*, 2012, **513**, 393.
30 H. Kawai, M. Tabuchi, M. Nagata, H. Tukamoto and A. R. West, *J. Mater. Chem.*, 1998, **8**, 1273.
31 R. D. Shannon, *Acta Crystallogr., Sect. A: Found. Crystallogr.*, 1976, **32**, 751.
32 K. F. Chen and D. F. Xue, *J. Phys. Chem. C*, 2013, **117**, 22576.
33 R. G. Burns, *Mineralogical Applications of Crystal Field Theory*, Cambridge University Press, Cambridge, 2nd edn, 1993.
34 D. T. Liu, C. Y. Ouyang, J. Shu, J. Jiang, Z. X. Wang and L. Q. Chen, *Phys. Status Solidi B*, 2006, **243**, 1835.
35 M. A. Mousa, A. M. Summan and M. A. Ahmed, *Thermochim. Acta*, 1990, **158**, 177.
36 D. C. Carter and T. O. Mason, *J. Am. Ceram. Soc.*, 1988, **71**, 213.
37 S. E. Dorris and T. O. Mason, *J. Am. Ceram. Soc.*, 1988, **71**, 379.

